Research on RIS Assisted Vehicle Communication Method Based on Deep Learning

Hua Tan, Chenguang He(✉), and Dezhi Li

School of Electronics and Information Engineering, Harbin Institute of Technology, Harbin 150001, China
1201051820@stu.hit.edu.cn, {hechenguang,lidezhi}@hit.edu.cn

Abstract. This thesis proposes an innovative system framework for vehicular communication utilizing Reconfigurable Intelligent Surfaces (RIS) to support millimeter-wave (mmWave) scenarios, addressing the high transmission rate demands of 6G communication. Due to significant path loss in mmWave propagation, RIS is introduced to enhance coverage and communication rates. Additionally, the thesis employs a deep learning-based Graph Neural Network (GNN) algorithm to optimize beamforming at the base station and phase shift matrices at the RIS, bypassing complex channel estimation processes. Simulation results demonstrate that the proposed algorithm exhibits excellent performance and generalization capabilities, enabling rapid response in vehicular communication scenarios.

Keywords: reconfigurable intelligent surface · deep learning graph neural network architecture · vehicle communication

1 Introduction

Advancements in mobile communication have equipped modern vehicles with capabilities for positioning, V2V communication, vehicle perception, autonomous driving, and intelligent transportation systems, enhancing traffic safety. Millimeter-wave (mmWave) communication, operating in the 30 GHz to 300 GHz range, meets the demand for higher transmission rates and throughput using advanced beamforming techniques to counter high propagation losses, achieving wireless data rates exceeding 6 GHz [1]. These technologies enable precise vehicle positioning, essential for autonomous driving [1,2].

However, urban environments with obstructions, reflections, and high vehicle mobility causing rapid channel changes can degrade communication links. Reliable communication requires strategic planning and infrastructure. Fast channel

This work is supported by the Key R&D Program of Heilongjiang Province under Grant JD22A001.

H.-H. Chen and W. Meng (Eds.): WiSATS 2024, LNICST 605, pp. 301–311, 2025.
https://doi.org/10.1007/978-3-031-86196-3_26

switching during vehicle movement affects communication quality and rate. Limited spectrum and hardware resources demand innovative methods to enhance performance by increasing data rates, reducing power consumption, and minimizing latency.

Reconfigurable Intelligent Surfaces (RIS) offer a solution for energy-efficient communication, mitigating high attenuation in mmWave and terahertz systems [3]. Comprising many independently controlled reflective elements, RIS enhances signal-to-noise ratio (SNR) at the receiver by adjusting the phase of reflected signals [5]. Placed between the base station and the target user, RIS redirects multipath signals to supplement the communication path when direct links are obstructed, creating passive beams aimed at the user. RIS can establish a smart radio environment (SRE) to address 6G network limitations [4].

A challenge in SRE-assisted vehicular communication is dynamically adjusting RIS elements in complex and variable channels. Each RIS element has an independent channel, requiring knowledge of the communication channel parameters for each antenna and reflecting element. Optimizing the reflected signal and enhancing SNR involves extensive, high-complexity computations [6].

To address this, this thesis introduces deep learning methods to accelerate optimization. Deep learning models, capable of extracting features from raw data, handle complex data and improve through parameter tuning [7]. They reduce computational complexity compared to traditional methods [8]. This thesis proposes a deep learning-based approach for RIS-assisted vehicular communication systems, training models on real-world datasets to enhance communication stability and reliability in high-mobility scenarios, thereby maximizing data rates.

2 System Model

This chapter designs a distributed RIS-assisted communication system, consisting of a base station (BS), which communicates with user equipment (UE) through direct links and RIS-cascaded links with the assistance of N distributed RISs ($R_n, n = 1, \ldots, N$). As shown in Fig. 2.

2.1 Communication Model for Reconfigurable Intelligent Surfaces

In this system, the nth Reconfigurable Intelligent Surface (RIS) consists of L passive reflective units capable of altering both the amplitude and phase of electromagnetic waves. Each RIS, regardless of its location, has the same number of reflective units. Both the transmitter and receiver employ single-antenna systems. The phase shift matrix at the nth RIS is denoted as $\Theta_n = \mathrm{diag}([k_{n1}e^{j\theta_{n1}}, \ldots, k_{nl}e^{j\theta_{nl}}, \ldots, k_{nL}e^{j\theta_{nL}}])$, where $k_{nl} \in (0, 1]$ and $\theta_{nl} \in [0, 2\pi)$ represent the amplitude reflection coefficient and phase shift of the lth reflective unit on the nth RIS, respectively (Fig. 1).

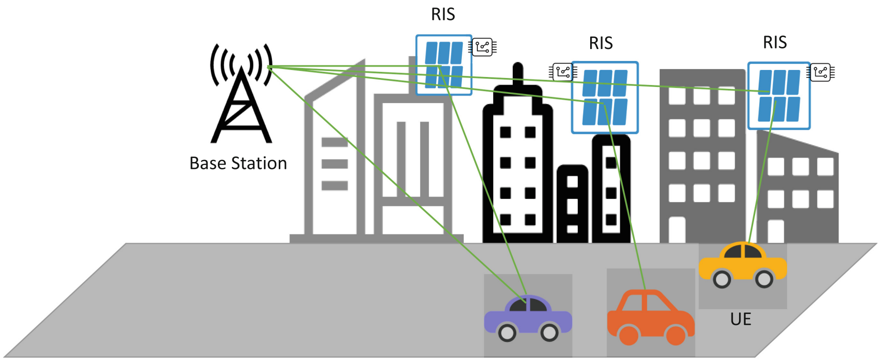

Fig. 1. System Model for Multi-RIS Assisted Communication

Each RIS is equipped with low-power communication and control modules to enable straightforward interaction with the base station, which handles the computation and distribution of phase shift matrices. RIS deployment ensures line-of-sight communication for both uplink and downlink channels, enhancing transmission rate and reliability by creating additional propagation paths and adjusting the phase of reflected waves. The base station, with perfect global Channel State Information (CSI), can directly compute and deploy the necessary phase shift matrices to the RISs. The single-antenna configuration at both transmitter and receiver simplifies optimization, facilitating easier validation of the performance of multiple RISs.

Define h_{nl} and g_{nl} as the complex channel coefficients from the base station to the nth reflective unit's lth reflection and from that reflective unit to the user equipment (UE), respectively. h_0 represents the channel coefficient of the direct link from the base station to the UE. x_S denotes the transmission symbol at the base station (with $E[|x_S|^2] = 1$), P_S is the transmission power at the base station (in dBm), and ω_D is the additive white Gaussian noise (AWGN) at the UE, with zero mean and variance σ_D^2, i.e., $\omega_D \sim \mathcal{CN}(0, \sigma_D^2)$.

As the user equipment (UE) employs a single antenna for signal reception, the signal takes the form of a direct superposition of all multipath signals. Consequently, the received signal at the UE is composed of both the direct signal and the reflected signals from all N Reconfigurable Intelligent Surfaces (RISs), and can be expressed in the form of Eq. (1).

$$y_r = \sqrt{P_S}\left(h_0 + \sum_{n=1}^{N}\sum_{l=1}^{L_n} g_{nl}k_{nl}e^{j\theta_{nl}}h_{nl}\right)x_S + \omega_D \tag{1}$$

Expressing the complex channel coefficients in polar coordinates, the Signal-to-Noise Ratio (SNR) received at the User Equipment (UE) location can be represented as Eq. (2).

$$SNR_r = \bar{\rho}\left|\left(h_0 e^{j\phi_0} + \sum_{n=1}^{N}\sum_{l=1}^{L_n} g_{nl} k_n h_{nl} e^{j(\theta_{nl}+\alpha_{nl}+\beta_{nl})}\right)\right|^2 \tag{2}$$

$$SNR_r = \bar{\rho}\left|\left(e^{j\phi_0}\right)\right|^2 \left|\left(h_0 + \sum_{n=1}^{N}\sum_{l=1}^{L_n} g_{nl} k_{nl} h_{nl} e^{j\delta_{nl}}\right)\right|^2 \tag{3}$$

$$SNR_r = \bar{\rho}\left|e^{j\phi_0}\right|^2 \left|h_0 + \sum_{n=1}^{N}\sum_{l=1}^{L_n} g_{nl} k_{nl} h_{nl} e^{j\delta_{nl}}\right|^2 \tag{4}$$

Here, $\bar{\rho} = \frac{P_S}{\sigma_D^2}$ represents the average transmit Signal-to-Noise Ratio (SNR) in dB, $\delta_{nl} = \theta_{nl} + \alpha_{nl} + \beta_{nl} - \phi_0$ denotes the phase error of the lth reflection element of the nth RIS relative to the direct link channel parameters. Since both the transmitter and receiver are single-antenna systems, the direct link channel conditions contain only one amplitude and phase information. Thus, the direct link channel can serve as a reference for designing the phase adjustment parameters for the reflection elements on the RIS.

Based on this analysis, the ideal phase shift configuration for the lth reflection element of the nth RIS can be represented as Eq. (5).

$$\theta_{nl}^{*} = \arg\max_{\theta_{nl}\in\mathcal{Q}} \mathrm{SNR}_r(\theta_{nl}), \quad \forall l \forall n \tag{5}$$

2.2 RIS-Assisted Communication Optimization Problem Modeling

Based on the aforementioned system model architecture, the Reconfigurable Intelligent Surface (RIS) is integrated into the vehicular communication system. This integration enables communication targets with high mobility to maintain good line-of-sight communication with the base station through the RIS. According to Shannon's formula, combined with the previously derived signal propagation paths and channel model, the achievable maximum rate R (bits/sec/Hz) of the communication target in this system architecture can be expressed as:

$$R = \log_2\left(1 + \bar{\rho}\left|e^{j\phi_0}\right|^2 \left|h_0 + \sum_{n=1}^{N}\sum_{l=1}^{L_n} g_{nl} k_{nl} h_{nl} e^{j\delta_{nl}}\right|^2\right) \tag{6}$$

Among them, $\bar{\rho}\left|e^{j\phi_0}\right|^2 \left|h_0 + \sum_{n=1}^{N}\sum_{l=1}^{L_n} g_{nl} k_{nl} h_{nl} e^{j\delta_{nl}}\right|^2$ represents the Signal-to-Noise Ratio (SNR) of the receiving user, and $\bar{\rho} = \frac{P_S}{\sigma_D^2}$ is the average transmission SNR. For ease of calculation, we consider the amplitude reflection coefficient of the RIS to be 1, and the phase error of the l-th reflecting element of the RIS is defined as $\delta_l \triangleq \theta_l + \alpha_l + \beta_l - \phi_0$. By optimizing the reflection coefficients, the above rate can be maximized, and the problem can be formulated as follows:

$$\delta_{nl}^{\star} = \arg\max\left(\log_2\left(1 + \bar{\rho}\left|h_0 + \sum_{n=1}^{N}\sum_{l=1}^{L_n} g_{nl} h_{nl} e^{j\delta_{nl}}\right|^2\right)\right) \tag{7}$$

3 RIS Implicit Channel Estimation Algorithm

The paper proposes using a neural network-trained model to represent the mapping function in an optimization problem. Extensive channel data, including transmitter pilot sequences, receiver signals, and known channel parameters, train the neural network. The objective is for the neural network to learn the mapping from received pilot signals to the RIS phase shift matrix and the base station's beamforming vector, maximizing network utility while bypassing the channel estimation stage.

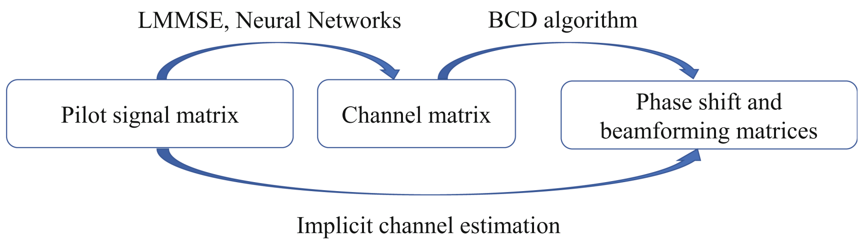

Fig. 2. Different algorithms

In multi-user cellular networks, addressing inter-user interference is critical, especially in dense environments, as it significantly impacts system performance, including user throughput and connection quality. To address this, we employ Graph Neural Networks (GNNs) to model and optimize user beamformers and reflection matrices. GNNs are adept at handling graph-structured data, facilitating effective learning of intricate relationships between network nodes.

We construct a graph with $K+1$ nodes representing users and an RIS, with edges depicting interactions symbolizing physical-layer assistance or interference. Each node is characterized by a vector z_k, where k denotes the node index. GNNs iteratively update node representation vectors through multiple layers to capture useful information. Using current node representations, GNNs apply graph neural network operations at each layer for iterative refinement.

By integrating beamformer and phase shift matrix collaboration at the RIS and leveraging GNNs for graphical representation and optimization, we manage inter-user interference, thereby enhancing network performance and capacity. This approach promises improved communication quality and user experience.

The GNN structure comprises three main layers: the initialization layer, the data separation and aggregation layer, and the normalization final layer. The initialization layer uses pilot signals as input, denoted as z_k^0. The data separation and aggregation layer aggregates and transmits information between nodes, yielding updated representation vectors z_k^d, where $d = 1, \ldots, D$. Finally, the linear layer generates $z_k^{(D+1)}$, mapped to beamformer matrices w_k and the phase shift matrix v through normalization. This architecture enables GNNs to flexibly adapt to problems of varying scales and complexities, effectively representing and learning graph structures through parameter sharing and feature extraction. The overall architecture is depicted in Fig. 3.

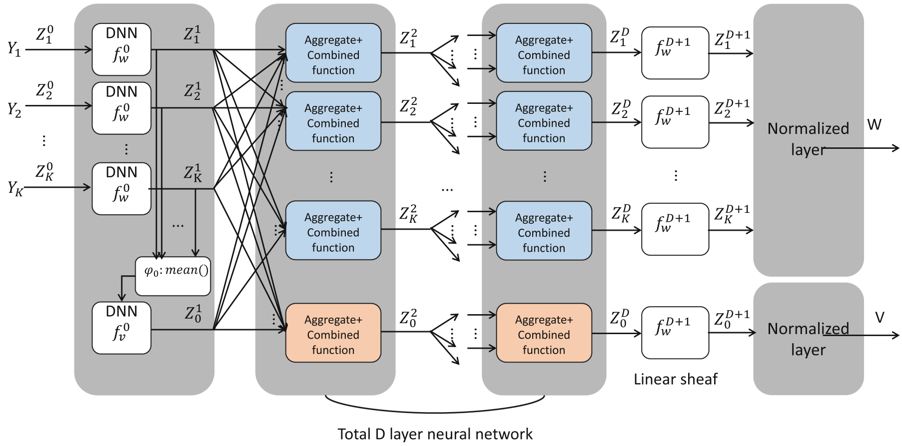

Fig. 3. Overall graph neural network architecture

3.1 Neural Network Training Parameter Setting

For the proposed 2-layer GNN with $D = 2$, where $k = 0, \ldots, 4$ and $d = 1, 2$. TensorFlow, a deep learning library, will be utilized to implement the proposed network. During the training process, the Adam optimizer will be employed to iteratively update the parameters, with an initial learning rate set to 10^{-3}. The learning rate will decrease by a factor of 0.98 after 300 iterations. In each training epoch, the parameters of the neural network will be updated through 100 iterations, and 1024 training samples will be used to compute the gradient at each iteration. The training process will terminate if the loss function does not significantly improve on the validation dataset over 10 consecutive training points.

3.2 Deep Learning Performance Analysis

Generate Training and Test Datasets. This paper focuses on a deep learning-based Reconfigurable Intelligent Surface (RIS) assisted vehicular communication system. In urban environments, vehicular communication faces significant challenges due to complex electromagnetic conditions and a high density of users, leading to substantial interference and channel blockages. Therefore, this research primarily targets urban communication scenarios. Given the mobility of vehicles, it is crucial to rapidly respond to changing channel conditions by synchronously updating the RIS reflection matrices and beamforming vectors following vehicle position updates.

The DeepMIMO dataset, published by the Information Theory and Applications Workshop, provides various scenarios, including indoor, outdoor, urban, and suburban settings. Each scene has distinct characteristics and channel properties, including channel matrices and Channel State Information (CSI), aligning well with the requirements of this study.

Using the DeepMIMO dataset involves two main steps: first, selecting and downloading the appropriate scenario and corresponding Python package from the official website; second, inputting scenario parameters to generate channel information. The general framework is depicted in Fig. 4. For this study, the "O1" outdoor ray-tracing scenario is chosen to generate channel information. This dataset operates at a frequency of 60GHz, which is within the millimeter-wave communication range.

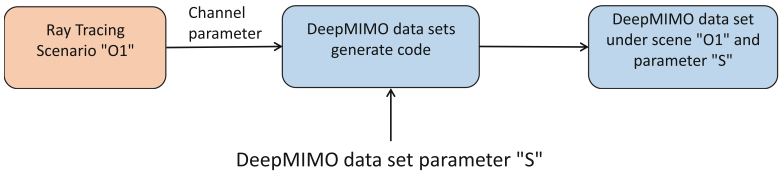

Fig. 4. Generate DeepMIMO dataset framework

The following Table 1 introduces the specific settings of the scenario used in this article.

Table 1. DeepMIMO dataset parameter setting

DeepMIMO dataset parameters	Numeric
Number of base station antennas	1,8,1
Number of RIS antennas	1,10,10
System bandwidth	100 MHz
Consider the number of strongest signal components	1
Antenna spacing	0.5λ

3.3 Performance Comparison of Different Algorithms

Next, the training data will be fed into the neural network, and the system performance will be evaluated against the following benchmarks during the testing phase:

Benchmark 1: Perfect CSI with BCD: Solving the rate maximization problem using block coordinate descent (BCD) algorithm with perfect CSI.

Benchmark 2: LMMSE Channel Estimation with BCD: Estimating channels using the LMMSE estimator, then employing the BCD algorithm for rate maximization.

Benchmark 3: Deep Learning-based Channel Estimation with BCD: Implementing a neural network for explicit channel estimation, followed by BCD-based design of phase shifts and beamformers. Comparing its performance against the proposed implicit channel estimation strategy in this paper to understand the advantages of implicit channel estimation over explicit channel estimation.

Firstly, in Fig. 5, the impact of the length of uplink pilots on downlink throughput and rate is demonstrated.

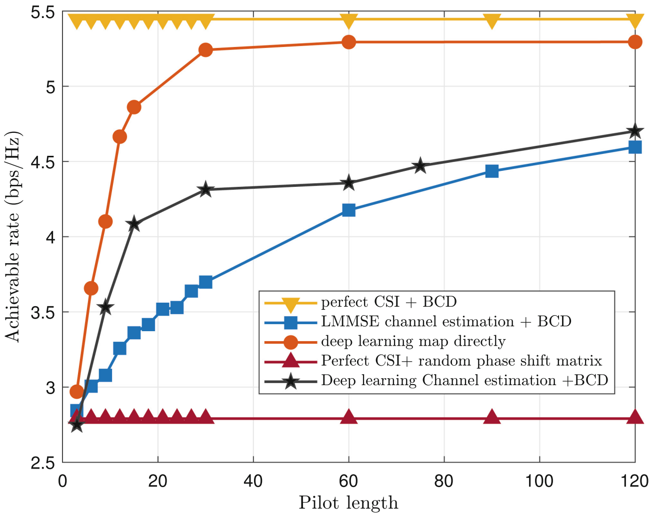

Fig. 5. Performance comparison of different algorithms

Figure 5 demonstrates that the BCD algorithm with perfect CSI (Benchmark 1) achieves the theoretical upper bound of the achievable rate. The deep learning approach proposed in this paper achieves approximately 90% of Benchmark 1's total rate with only 40 pilot signals, with further increases in pilot signals resulting in marginal rate improvements. In contrast, traditional explicit channel estimation methods (Benchmarks 2 and 3) require at least 120 pilot signals to achieve similar rates. While the deep learning algorithm initially requires longer training, its direct mapping for channel estimation is faster than the LMMSE algorithm once trained. Overall, the GNN architecture effectively learns the mapping from pilot signals to optimization, significantly reducing pilot training costs.

Next, we will compare the computational time of different algorithms. In vehicular communication, rapid channel changes necessitate real-time adjustments by the RIS, requiring high computational efficiency from optimization algorithms. We will calculate the total time spent by each algorithm for 1000 sample data points under various pilot signal scenarios.

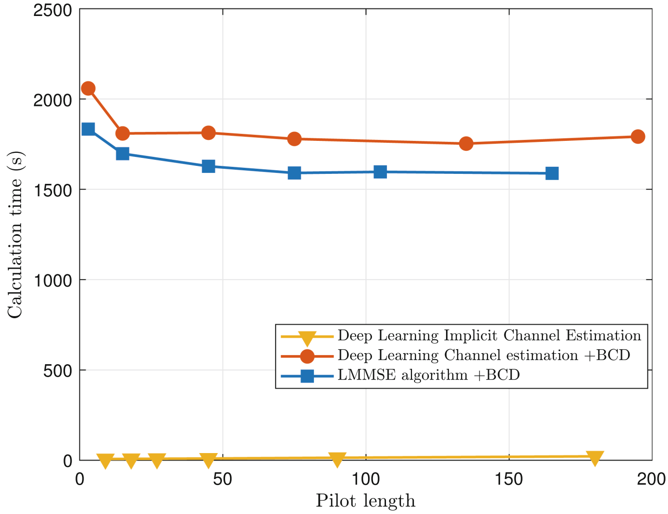

Fig. 6. Comparison of time consumption of different algorithms

Figure 6 demonstrates that, with a trained deep learning model, the time required for beamforming vector and phase shift matrix calculations significantly decreases compared to using the BCD algorithm. Deploying deep learning models at the BS enables rapid adjustment of the RIS phase shift matrix for vehicles entering a specific area, enhancing communication quality. However, as the length of pilot signals increases, the computational time for deep learning-based implicit channel estimation also increases due to the larger input vectors, while the BCD algorithm converges faster with longer pilot signals.

To evaluate the generalization capability of the GNN model and to compare user performance at different distances from the RIS and BS, we consider a scenario where a vehicle gradually approaches a high-demand communication intersection. In the DeepMIMO dataset, only the data from the intersection center is used for training, while the test dataset includes users at various positions. The pilot signal is input into the trained neural network to obtain the achievable rate. The simulation results are shown in Fig. 7, where the 50 m in the simulation parameters represent the center of the intersection. This area is unobstructed with strong signals, while the range from 0 to 150 m depicts the process of moving from a heavily obstructed area into the intersection center and then driving away.

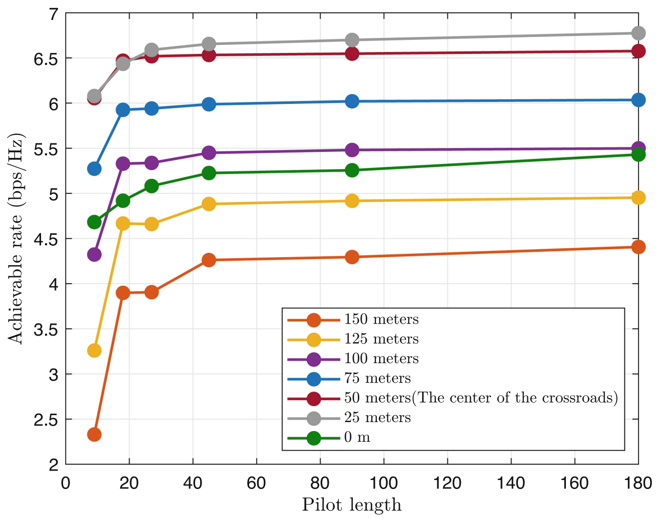

Fig. 7. Relationship between user distance and achievable rate

The simulation results indicate that as the vehicle approaches the intersection from a farther distance, the communication rate gradually increases when using the model trained with the intersection position data. This suggests that deploying the model at the current intersection can effectively enhance communication rate and stability as vehicles enter high-demand communication intersections. Performance is notably good at both 25 m and 75 m. Additionally, when the vehicle is in a heavily signal-blocked area, appropriately increasing the length of the pilot signal can significantly improve the achievable rate, addressing the millimeter-wave blockage issue.

4 Conclusion

This study focuses on a deep learning-based approach for RIS-assisted vehicular communication systems. Throughout this process, a system model for RIS-assisted communication is established, and the performance of deep learning algorithms is compared under different conditions.The research findings are summarized as follows:

Based on the RIS-assisted communication system architecture, a model for deep learning optimization problems is developed. The model is trained using appropriate datasets and tested against traditional algorithms. Results show that the deep learning method closely approximates the theoretical achievable rate upper bound with minimal training costs, exhibiting superior performance. Additionally, in vehicular communication scenarios, the method responds rapidly to vehicle channel switching and effectively enhances achievable rates and stability in high-demand communication areas.

References

1. Lavdas, S., Gkonis, P.K., Tsaknaki, E., Sarakis, L., Trakadas, P., Papadopoulos, K.: A deep learning framework for adaptive beamforming in massive mimo millimeter wave 5g multicellular networks. Electronics 1**2**(17), 3555 (2023)
2. Hashida, H., Kawamoto, Y., Kato, N.: Intelligent reflecting surface placement optimization in air-ground communication networks toward 6g. IEEE Wirel. Commun. **PP**(99), 1–6 (2020)
3. Bjornson, E., Ozdogan, O., Larsson, E.G.: Reconfigurable intelligent surfaces: three myths and two critical questions. IEEE Commun. Mag. **58**(12), 90–96 (2020). https://doi.org/10.1109/MCOM.001.2000407
4. Di Renzo, M., et al.: Smart radio environments empowered by reconfigurable intelligent surfaces: How it works, state of research, and the road ahead. IEEE J. Selected Areas Commun. 38(11), 2450–2525 (2020)
5. Albinsaid, H., Singh, K., Biswas, A.B.S., et al.: Multiple antenna selection and successive signal detection for smbased irs-aided communication. IEEE Signal Process. Lett. **28**, 813–817 (2021)
6. Wang, Z., Liu, L., Cui, S.: Channel estimation for intelligent reflecting surface assisted multiuser communications: Framework, algorithms, and analysis[J]. IEEE Trans **19**(10), 6607–6620 (2020)
7. Jia, C., Gao, H., Chen, N., et al.: Machine learning empowered beam management for intelligent reflecting surface assisted mmwave networks. China Commun. **17**(10), 100–114 (2020)
8. Kadhim, J.Q., Sallomi, A.H.: Enabling deep learning and swarm optimization algorithm for channel estimation for low power RIS assisted wireless communications. Int. J. Interact. Mobile Technol. (iJIM) (2023)